Colloid Polym Sci (2005) 284: 192–202
DOI 10.1007/s00396-005-1360-z

ORIGINAL CONTRIBUTION

**Chueh-Jung Huang**
**Fuh-Sheng Shieu**

# Micellization and morphological characterization of Ag-micelles prepared by poly(vinyl acetate)–silver nitrate in solvent/nonsolvent system

Received: 31 January 2005
Accepted: 18 May 2005

C.-J. Huang · F.-S. Shieu
Department of Materials Engineering,
National Chung Hsing University,
250, Kuo Kuang Road, Taichung 402,
Taiwan, R.O.C

C.-J. Huang (✉)
Department of Chemical Engineering,
Hsiuping Institute of Technology, No.11,
GungYe Road, Dali City, Taichung 412,
Taiwan, R.O.C
E-mail: cjhcyy@ms57.hinet.net
Tel.: +886-4-23766311
Fax: +886-4-22857017

**Abstract** The inducing method for preparing Ag-micelle solution with the use of mixed solvent/nonsolvent, and the morphological characterization of the generated metal–micelles were investigated and reported in this paper. In this method, an Ag containing metal chelate polymer (MCP) raw solution was preprepared by dissolving poly(vinyl acetate) (PVAc)–silver nitrate ($AgNO_3$) MCP in conc. formic acid, and a mixed solvent of $HCOOH/H_2O$ with specific water composition was then added to induce the micellization of the MCP chain. The critical water concentration (CWC) that was needed for inducing the formation of the Ag-micelles, and the water concentration at which the flocculation of the Ag-micelles occurred in micellar solution, were studied by measuring the transmittance of the dilute MCP solution; the results showed that a long-lasting MCP solution with stable micelles might be prepared by using a $H_2O$/HCOOH solvent of specific weight ratio 1:1.2. The effect of the $AgNO_3$ concentration on the morphology of the Ag-micelles was also investigated by transmission electron microscopy (TEM). At $AgNO_3$ concentration below 0.5 wt%, the Ag-micelles displayed a variety of core-shell structure; but as the $AgNO_3$ concentration was increased to 1.0–2.0 wt%, micelles that had Ag-solid embedded in the micellar core were observed.

**Keywords** Ag-containing micelle · Poly(vinyl acetate) · Micellization · Morphology · Solvent/nonsolvent

## Introduction

Amphiphilic co-polymer, a surface-active macromolecule, with its polymer backbone consisting of hydrophobic and hydrophilic segments and with an ability to undergo micellization in a selective solvent, is of importance in preparing metal-containing micelles [1–11]. Many techniques developed for synthesizing metal–micelles have been reported in literature, and amongst them two typical methods that utilize the amphiphilic property of co-polymer are mostly adopted. One common method is to disperse the amphiphilic co-polymer into a nonpolar organic solvent and it starts micellization when the critical micelle concentration (CMC) is reached. The micelles generated are classified as the reverse type, i.e., the hydrophobic segment of the co-polymer aligns toward the organic solvent to form the micellar corona, whereas the hydrophilic segment of the co-polymer concaves inward to get away from the organic solvent and becomes the micellar core. If a chosen metal salt is added into the micelle solution, the metal ions can diffuse into the micellar core to form a complex with the hydrophilic groups, and after in situ reduction by adding an adequate reducing agent, these metal ions can be reduced to a metal which is embedded in micellar core to form the metal-containing micelles. Mayer et al. [10] used this method to prepare small metal-containing micelles of poly(styrene)-b-poly(ethylene oxide)-noble metal, which displayed variant morphologies described as cherry (one central particle), raspberry (multiple internal particles) and strawberry (small metal particles surrounding hydrophobic micelle core). This method was also used to prepare stable colloid in organic medium [2, 3, 12, 13].

Another method is to induce micellization of copolymer via reduction of its solubility. A presynthesized metal containing amphiphilic co-polymer is first dissolved in a good solvent, then a nonsolvent, usually $H_2O$, is added to reduce the solubility of the copolymer's hydrophobic segment, so that the metal-containing copolymer is induced to undergo micellization for ridding of water molecules. The nonsolvent concentration or the water content that was needed to induce the micellization is called the critical water concentration (CWC) [4, 14–16]. Micelles of pure amphiphilic co-polymer (without metal existing) prepared by this method have been studied, for example, Eisenberg [15] described the morphologies of crew-cut micelles formed by poly(styrene)-b-poly(acrylic acid) in aqueous solution as spheres, rods, lamella, vesicles, and complex aggregates. The inducing method has an advantage of using less amount of organic solvent compared to the aforementioned one, and the micelles that generated are of normal type bound with metal, i.e., the hydrophobic segment aligns inward and the metal-attached hydrophilic segment arranges outward. This structure has a drawback of exposing the attached metal outside the region of micellar corona, and the metal–micelles so formed are less stable and prone to aggregation in aqueous environment. Nevertheless, this shortcoming can be effectively overcome by dissolving the presynthesized metal–amphiphilic polymer with a mixed solvent/nonsolvent [6, 17–19].

The underlying principle for these two methods is summarized as follows: if a polymer has both hydrophilic and lipophilic parts in its structure, such as the amphiphilic co-polymer, then it may possess the surface-active properties, so that by self-orientation it can expose its hydrophilic moieties into the water phase and turn its hydrophobic regions into the lipophilic environment; therefore it may undergo micellization in a selective medium, and it may be used to prepare a stable metal–micelle solution [20].

In our previous studies [21], we synthesized Ag-PVOH/PVAc, denoted as MCP (metal chelate polymer), by adding silver nitrate ($AgNO_3$) to a solution of homogeneous polyvinyl acetate (PVAc) that predissolved in formic acid (HCOOH). The added $Ag^+$ ions were reduced by HCOOH to Ag(0) metal that formed complex with the PVAc, and at the same time some ester groups of the homo-PVAc backbone were hydrolyzed to hydroxyl groups (OH) so that the MCP (Ag-PVOH/PVAc) were obtained. Since the amphiphilicity of the PVOH/PVAc structure was higher than that of the homo-PVAc, one would expect a ready micellization of MCP by the inducing method of adding a mixed solvent/nonsolvent. In the present study, we thus extended our investigation on the micellization ability of the MCP by dissolving it in HCOOH, a good solvent for PVOH/PVAc, to form the MCP raw solution, a mixed solvent of HCOOH/$H_2O$ (solvent/nonsolvent) was then added to induce the micellization. The CWC was determined by measuring the UV transmittance of the micellar solution, and the surface-active properties were compared with between the homo-PVAc and the MCP. The morphological characterization of the Ag-micelles generated by varying the $AgNO_3$ concentration in the MCP raw solution was also investigated with the transmission electron microscopy (TEM).

## Experimental

### Preparation of MCP raw solutions with variant $AgNO_3$ concentration for MCP micelle solutions

To investigate the effect of $AgNO_3$ concentration on the morphology of the Ag-micelles, five MCP raw solutions having $AgNO_3$/PVAc weight ratios (wt%) of 0.1, 0.3, 0.5, 1.0, and 2.0 were prepared, respectively. To prepare these raw solutions, MCP products containing the specific weight ratio of $AgNO_3$ were obtained beforehand by dissolving PVAc (Kanto Chemical Co., Japan) in concentrated formic acid (>90.0%, Nacalai Tesque Inc., Japan) to form a 25 wt% PVAc/HCOOH solution, and a calculated amount of silver nitrate (Merck-Schuchardt Chemical Co., USA) that met the required $AgNO_3$/PVAc weight ratio was added to this solution. The resultant mixture was stirred at 45°C in air for several hours and then poured into a large amount of distilled water (1,000 ml) to precipitate out the MCP. The MCP precipitate was filtered out and dried to form the required MCP product. It is to be noted that the MCP product which contained 0.5 wt% $AgNO_3$, denoted MCP0.5, was also used in the preparation of dilute MCP0.5/HCOOH sample solution for the CWC measurement described in the next section.

The five MCP raw solutions of different $AgNO_3$ concentrations were prepared, respectively, by re-dissolving 3 g of the specific MCP product in 7 g formic acid, the good solvent, so that the composition of each MCP raw solution was 30 wt% MCP/70 wt% HCOOH. All the prepared MCP raw solutions were sealed in different sample vases for later use in the preparation of MCP micelle solutions.

The pH value of these MCP raw solutions was less than 0.01 and their compositions are listed in Table 1. The MCP product character; FTIR frequency ($cm^{-1}$): 1,738 [$\nu_s$, C=O], 1,241 [$\nu_a$, C–O–C], 1,022 [$\nu$, CH–O] and weak band near 3,500 [OH bonding]; $^{13}$C-NMR in DMSO-d6,δ(ppm):169.7 [carbonyl,$\underline{C}=O$], 67.9 [methine,$\underline{C}$(mm)–$OCOCH_3$], 67.0/66.6/66.3 [methine,$\underline{C}$(mr)–$OCOCH_3$], 65.9 [methine,$\underline{C}$(rr)–$OCOCH_3$], 63.5 [methine,$\underline{C}H$–OH], 42.6/42.3/42.1/42.0 [methylene,$\underline{C}H_2$–CH–OH], 38.7/38.5/38.3/38.0 [methylene,$\underline{C}H_2$–$CHOCOCH_3$], 20.7 [methyl,$\underline{C}H_3$]; XRD, difference angles (2θ) and plane distance (*d*): 38.10/2.36 [Ag(111)], 44.27/2.04 [Ag(200)], 64.41/1.44 [Ag(220)], and 77.45/1.23 [Ag(311)].

### Preparation of dilute PVAc/HCOOH and MCP/HCOOH solutions for CWC measurement

For CWC measurement, a set (A) of three dilute PVAc/HCOOH solutions, denoted 1.0 wt% PVAc/99.0 wt% HCOOH, 2.0 wt% PVAc/98.0 wt% HCOOH, and 3.0 wt% PVAc/97.0 wt% HCOOH, were prepared by dissolving 1, 2, and 3 g of the pure PVAc into conc. formic acids of 99, 98, and 97 g, respectively. Another set (B) of three dilute MCP0.5/HCOOH solutions, denoted 1.0 wt% MCP0.5/99.0 wt% HCOOH, 2.0 wt% MCP0.5/98.0 wt% HCOOH, and 3.0 wt% MCP0.5/97.0 wt% HCOOH, were also prepared by dissolving 1, 2, and 3 g of the MCP0.5 product into conc. HCOOH acids of 99, 98, and 97 g, respectively. The transmittance of these six solutions was measured with a UV/VIS Spectronic 20D Series Spectrophotometer at a wavelength of 450 nm according to the standard procedure: (1) Take 10 g of the dilute solution as the testing sample. (2) Add 0.1 ml distilled water to the testing sample and record the water content. (3) Stir the resultant sample solution and then settle for 10 min to establish a stable turbidity. (4) Measure the transmittance of turbid sample solution three times and take the averaged value. (5) Repeat from step (2) until the transmittance of the sample solution presented two reflection points. At the first reflection point, the values of the measured transmittance will change pattern from acute descending to slow leveling, and the second reflection point is a point at which the measured values starts ascending again. (6) Then plot in a graph the measured transmittance (%) against the recorded water content (ml) for CWC analysis.

### Preparation of the MCP micelle solutions

The MCP micelle solutions with variant contents of PVAc, $AgNO_3$ and water used for this study are summarized in Table 1. To prepare these MCP micelle solutions, a mixed solvent of $HCOOH/H_2O$ was added to the afore-prepared MCP raw solutions, and followed with a 1-h vigorous stirring for complete micellization. The weight ratio of water to formic acid in the mixed solvent was specified as 1:1.2 (w/w, $H_2O$ 45.45 wt% and HCOOH 54.55 wt%) to ensure that the water content added was greater than the CWC value needed to induce micellization. Also, the added amount of mixed solvent was calculated such that the polymer concentration in the resultant MCP micelle solution was attenuated from 30 wt% to about 1.0–3.0 wt%.

**Table 1** Composition of MCP raw solution and MCP micelle solution

| MCP raw solution (30 wt% MCP/70 wt% HCOOH) | | MCP micelle solution $PVAc/HCOOH/H_2O$ |
|---|---|---|
| Sample | $AgNO_3$ content[a] (wt%) | [*x* wt%/*y* wt%/*z* wt%][b] |
| MCP0.1 | 0.1 | 3.8/50.0/46.2 |
| MCP0.3 | 0.3 | 3.6/50.0/46.4 |
| MCP0.5 | 0.5 | 2.7/50.0/47.3 |
| MCP1.0 | 1.0 | 1.8/50.0/48.2 |
| MCP2.0 | 2.0 | 1.0/50.0/49.0 |

[a] The weight percentage (wt%) of $AgNO_3$ with respect to 30 g PVAc in the MCP product

[b] *x*, *y*, and *z* represent the composition of PVAc, HCOOH and $H_2O$, respectively, in the micelle solution. The specific gravity is 1.2 for HCOOH and 1.0 for water

Before performing the TEM analysis, the MCP micelle solution was vibrated for 20 s by an ultrasonic vibrator. A drop of this solution was then taken and placed on a formval/carbon-coated copper grid for complete vaporization of solvent. The dried specimens of all MCP micelle solutions were examined by a Zeiss ME 902A TEM operated at 80 kV.

## Discussion

### The CWC and the water concentration range (WCR)

As described in the Introduction of this paper, an addition of water into the dilute MCP/HCOOH system would induce the micellization of MCP to form micelles in the system. Before the CWC, a white cloudy flocculus was observed the instant when water was added into the dilute MCP/HCOOH solution, but the flocculus entirely disappeared after stirring or standing. This demonstrated that the micelles generated from MCP chains would be re-dissolved to free polymer chains when the added water content was less than the CWC values. However, when the added water content reached the CWC value, an acute increase in the turbidity happened and this turbidity phenomenon remained despite stirring or still standing. To obtain reliable data of the transmittance, we waited about 10 min until the solution reached a stable turbidity or fluctuation of transmittance data reached equilibrium, then measured the transmit-

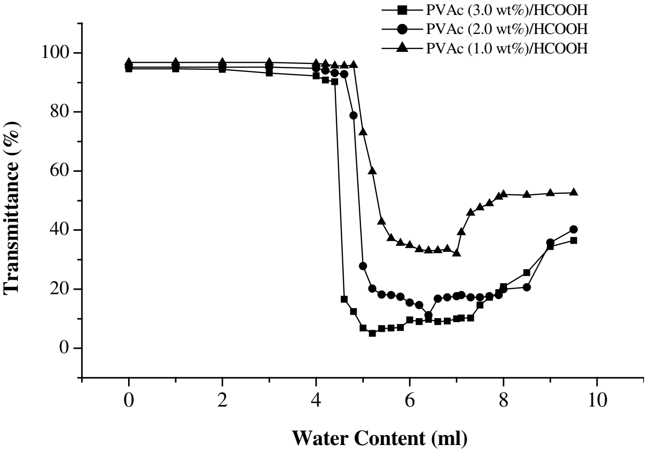

**Fig. 1** Effect of water content (ml) on the transmittance of the dilute PVAc/HCOOH solution: *filled triangle* for 1.0 wt% PVAc/99.0 wt% HCOOH, *filled circle* for 2.0 wt% PVAc/98.0 wt% HCOOH, and *filled square* for 3.0 wt% PVAc/97.0 wt% HCOOH

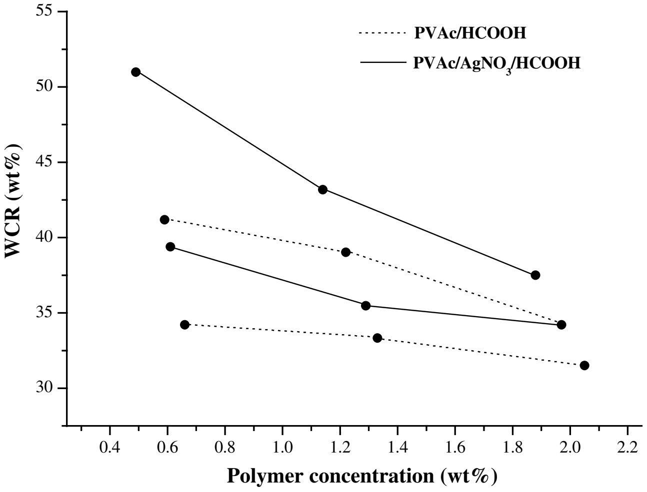

**Fig. 3** A plot of water concentration range (WCR) versus polymer composition: *broken line* for PVAc/HCOOH and *solid line* for MCP0.5/HCOOH

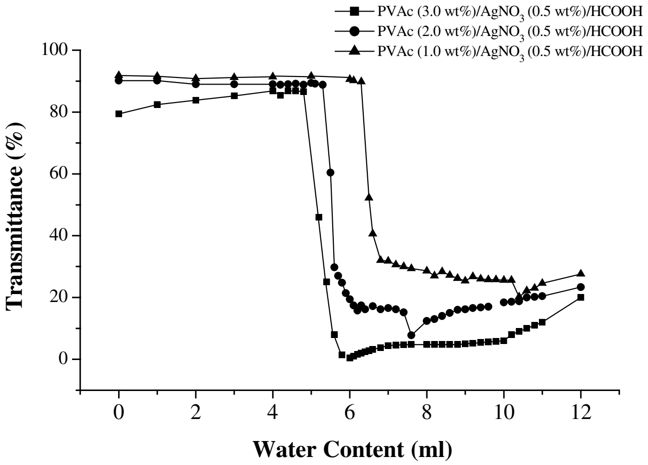

**Fig. 2** Effect of water content (ml) on the transmittance of the dilute MCP/HCOOH solution: *filled triangle* for 1.0 wt% MCP0.5/99.0 wt% HCOOH, *filled circle* for 2.0 wt% MCP0.5/98.0 wt% HCOOH, and *filled square* for 3.0 wt% MCP0.5/97.0 wt% HCOOH

tance data three times and took the average as the experimental value.

The CWC values, determined from Fig. 1 at the points showing abrupt decrease in transmittance, were 5.2, 5.0, and 4.6 ml for the 1.0, 2.0, and 3.0 wt% PVAc/HCOOH solutions, respectively. The results for dilute MCP0.5/HCOOH solutions show a similar pattern in Fig. 2, and from which the determined CWC values were 6.5, 5.5, and 5.2 ml for the 1.0, 2.0, and 3.0 wt% MCP0.5/HCOOH solutions, respectively. These CWC values indicate that the higher the concentration of polymer in the system, the lower the $H_2O$ content required to induce micellization. An interpretation for this is: the polymer chains would have weaker intermolecular forces at low polymer concentration, which needed more $H_2O$ molecules to induce their hydrophobic parts to keep closer for micellization.

The transmittance curves, as shown in Figs. 1 and 2, illustrate an acute descending when the water reached the CWC. According to the Flory-Huggins theory [1], in this initial stage the micelles would be mainly formed by polymer chains of larger molecular weight, but with a continuous increase in water content, small polymer chains were also induced to start micellization, and this increasing number of micelles made the transmittance descending. After all polymer chains had eventually transformed to micelles (i.e., the micelles' number or concentration reached the maximum), further addition of water merely attenuated the concentration of the micelles in the system solution, and this made the transmittance slightly ascended to reach the first reflection point. The first reflection points were at 7.0, 6.4, and 5.2 ml for the 1.0, 2.0, and 3.0 wt% PVAc/HCOOH systems; and were at 10.4, 7.6, and 6.0 ml for the 1.0, 2.0, and 3.0 wt% MCP0.5/HCOOH systems, respectively. If the water content corresponding to the descending range of transmittance, that is, the amount of water added between the CWC point to the first reflection point is plotted against the polymer composition of these system solutions, then the curves of water concentration range (WCR) are obtained, as shown in Fig. 3. Since the MCP chains contained hydroxyl groups in their PVOH/PVAc structure, which enables them to have a higher water affinity compared to the homo-PVAc chains, therefore, at the same polymer concentration, the CWC value of the MCP/HCOOH system

**Table 2** The water concentration range (WCR) and the composition of the dilute PVAc/HCOOH and MCP0.5/HCOOH solutions

| | $H_2O$ composition | | PVAc/HCOOH composition (wt%) | pH[b] |
|---|---|---|---|---|
| | (ml) | (wt%) | | |
| PVAc/HCOOH[a] (wt%) | | | | |
| PVAc(1.0)/HCOOH(99.0) | 5.2–7.0 | 34.21–41.18 | (0.66–0.59)/(65.13–58.23) | 0.08–0.23 |
| PVAc(2.0)/HCOOH(98.0) | 5.0–6.4 | 33.33–39.02 | (1.33–1.22)/(65.33–59.76) | 0.06–0.18 |
| PVAc(3.0)/HCOOH(97.0) | 4.6–5.2 | 31.51–34.21 | (2.05–1.97)/(66.43–63.82) | 0.05–0.08 |
| MCP0.5/HCOOH[a] (wt%) | | | | |
| PVAc(1.0)/HCOOH(99.0) | 6.5–10.4 | 39.39–50.98 | (0.61–0.49)/(60.00–48.53) | 0.20–0.60 |
| PVAc(2.0)/HCOOH(98.0) | 5.5–7.6 | 35.48–43.18 | (1.29–1.14)/(63.23–55.68) | 0.09–0.36 |
| PVAc(3.0)/HCOOH(97.0) | 5.2–6.0 | 34.21–37.50 | (1.97–1.88)/(63.82–60.62) | 0.08–0.12 |

[a] 10 g of dilute solutions were used. The pH values of all the sample solutions are below 0.01

[b] The pH values of the dilute solutions in the water concentration range

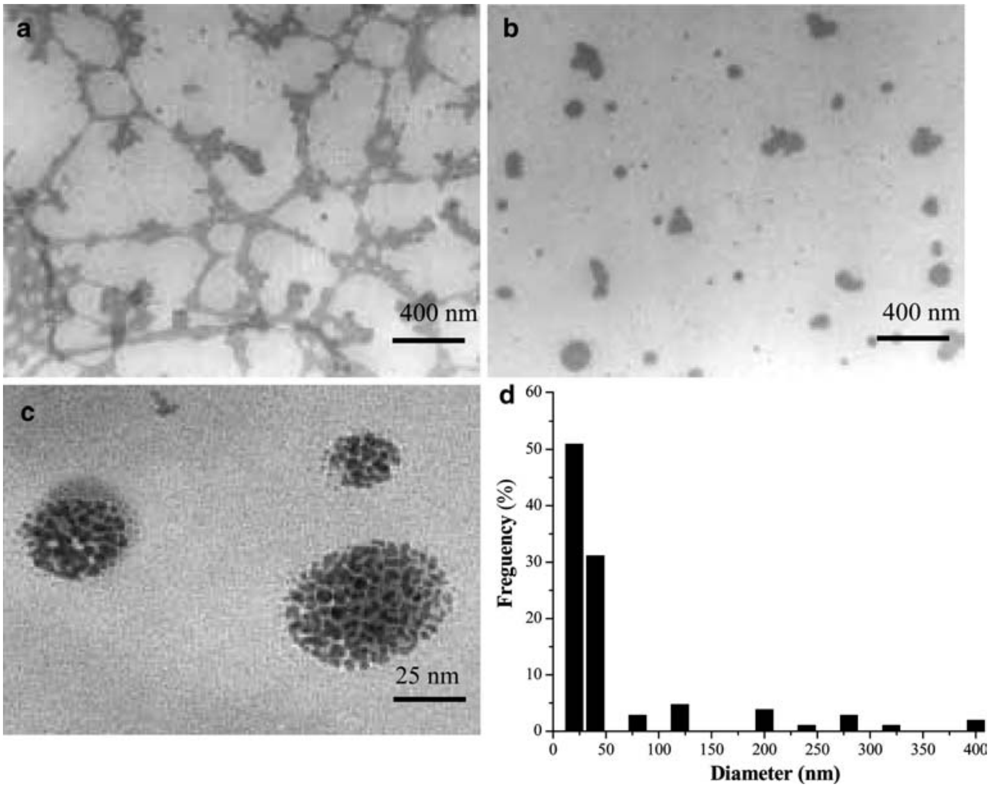

**Fig. 4** TEM images of dried specimens of homo-PVAc raw solution added with HCOOH/$H_2O$ mixed solvent, cast on a formval/carbon-coated copper grid. **a** 3.0 wt% PVAc/75 wt% HCOOH/22 wt% $H_2O$ with water content below the CWC range; **b** 3.0 wt% PVAc/50 wt% HCOOH/47 wt% $H_2O$ with water content exceeded the WCR; **c** Magnified image of (**b**); and **d** the particle size distribution of (**b**)

was higher than that of the homo-PVAc/HCOOH system, as shown in Fig. 3. This indicates that higher water content was needed to induce micellization in the MCP/HCOOH than the homo-PVAc/HCOOH. The WCR for both systems are listed in Table 2.

These micelle solutions were stable and the large associated aggregates of micelles would not occur until the water content reached the second reflection point. As shown in Figs. 1 and 2, the water content at the second reflection point is near 7.0 ml (41.18 wt%) for the PVAc/HCOOH system, and is about 11.0 ml (52.38 wt%) for the MCP/HCOOH system. When the added water content exceeded the second reflection point, the solvent quality became poorer for the hydrophobic segment, and an increase in the interfacial tension resulted [15]. The micelles of the system tend to associate together so as to diminish the total interfacial area. The fusion of micelles led to a reduction of their total numbers and an increase in the micellar radius; this not only destroyed the stability of the system, but also

**Fig. 5** TEM images of dried specimens of MCP micelle solutions, cast on a formval/carbon-coated copper grid, and the particle size distribution. **a** MCP0.1; **b** MCP0.5; and **c** MCP2.0

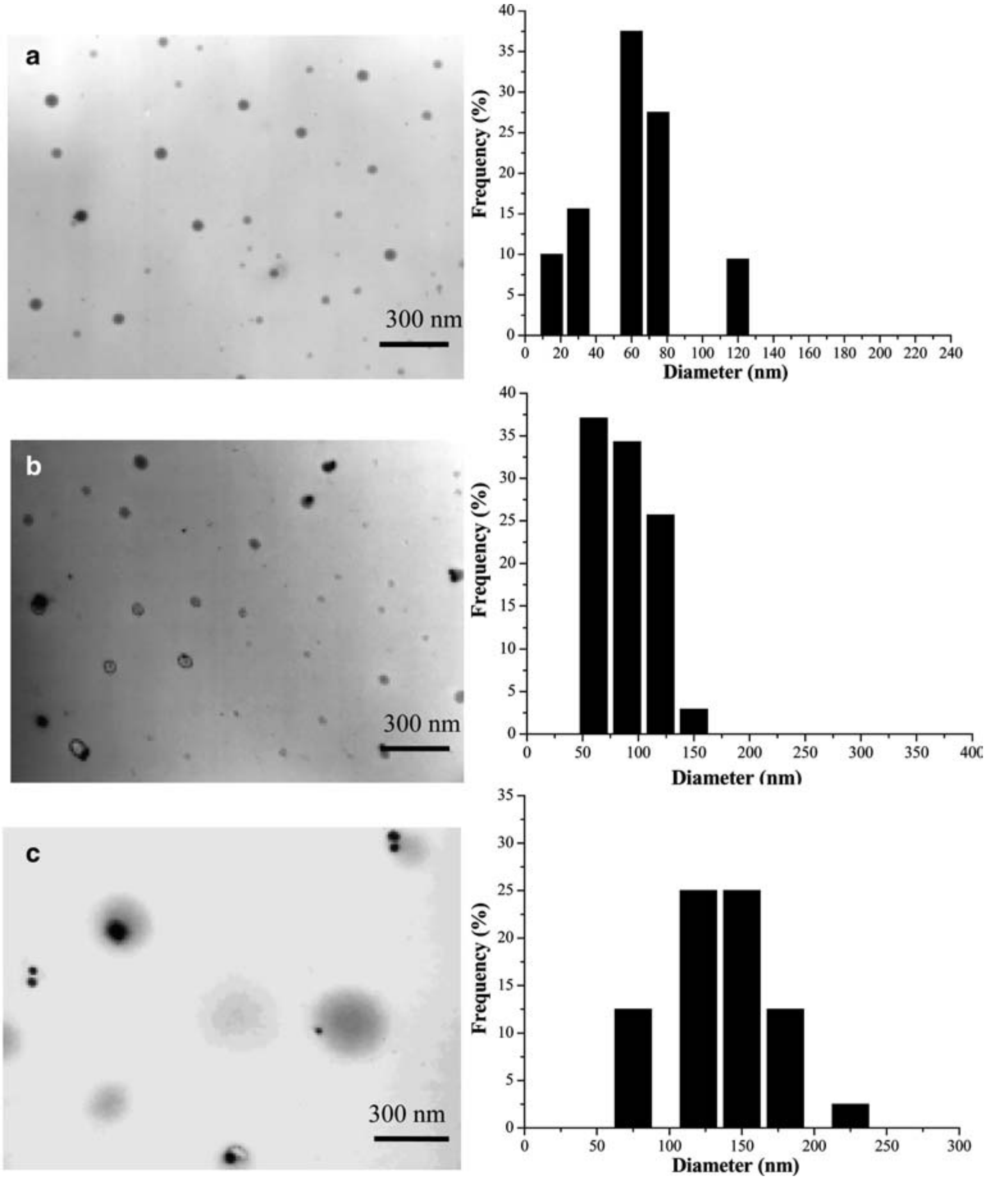

caused the precipitation of large-sized micellar aggregates. Thus, it is apparent that the transmittance of these solutions was raised after the water content exceeded the second reflection point.

Based on the above analysis, we can then prepare long-lasting and stable micelle solutions by controlling the proportion of water to the formic acid in the mixed solvent. In this study, the mixed solvent of $H_2O$/HCOOH used to induce the MCP raw solutions was kept in a ratio of 1:1.2 (45.45 wt% $H_2O$ and 54.54 wt% HCOOH), so that the water compositions of the MCP0.1, MCP0.3, MCP0.5, MCP1.0, and MCP2.0 micelle solutions were maintained at 46.2, 46.4, 47.5, 48.2, and 49.0 wt%, respectively, that is, between their first and second reflection points, to ensure a complete micellization and high stability of the resultant micelle solutions.

## The morphological features of Ag-micelles

A study on the microstructure of homo-PVAc is needed for comparing the effect of $AgNO_3$ on the morphology of MCP micelles. Figure 4 shows the TEM micrographs of dried specimens prepared from homo-PVAc raw solution induced with mixed HCOOH/$H_2O$ solvent. Figure 4a is the TEM image of the specimen prepared from a solution of 3.0 wt% PVAc/75.0 wt%

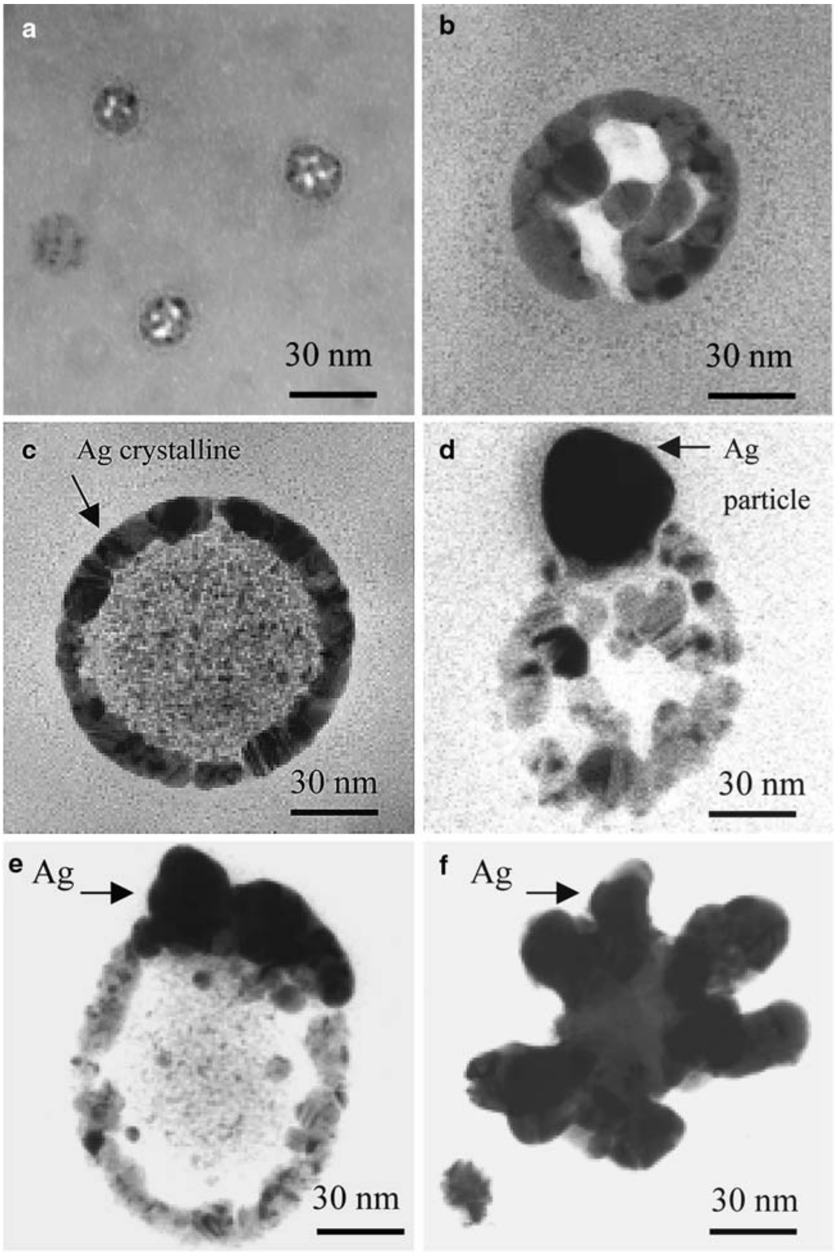

**Fig. 6** TEM images of dried specimens of MCP micelle solutions, cast on a formval/carbon-coated copper grid. MCP0.1: **a** vesicle micelle; MCP0.3: **b** vesicle micelle and **c** ring-like micelle; MCP0.5: **d** ring-like micelles, **e** ring-like micelle, **f** star-like micelle and **g** the SAD pattern of the polycrystalline Ag (0) in (**f**); MCP1.0: **h** sphere micelle, and **i** spherical micelle deformation; MCP2.0: **j** sphere micelle and **k** solid-core micelle

HCOOH/22.0 wt% $H_2O$, the water content added was less than the CWC value. It can be seen that the PVAc polymer displayed the image of an interconnected network. In Fig. 4b, the water adding exceeded the CWC, a solution of 3.0 wt% PVAc/50.0 wt% HCOOH/47.0 wt% $H_2O$ was formed and the PVAc polymer became aggregated. Being affected by their hydrophobic properties and the absence of any surfactant, the molecules of the homo-PVAc were difficult to disperse uniformly in the aqueous solution. They were liable to form droplet aggregates with irregular shapes and broad size distribution. The size of these aggregates ranged from smaller than 25 nm to larger than 400 nm, as shown in Fig. 4d. An enlargement of these aggregates displaying grainy structure is shown in Fig. 4c.

Figure 5 shows the microstructure of Ag-micelles, generated in an MCP raw solution induced with a mixed solvent of $H_2O$/HCOOH in weight ratio of 1:1.2 and seem to have a spherical shape under this low magnification. These MCP micelles have a narrower particle size distribution compared to the micelles of PVAc system shown in Fig. 4b. Figure 6a is an enlarged TEM showing the microstructure of Ag-micelles prepared

**Fig. 6** (Contd.)

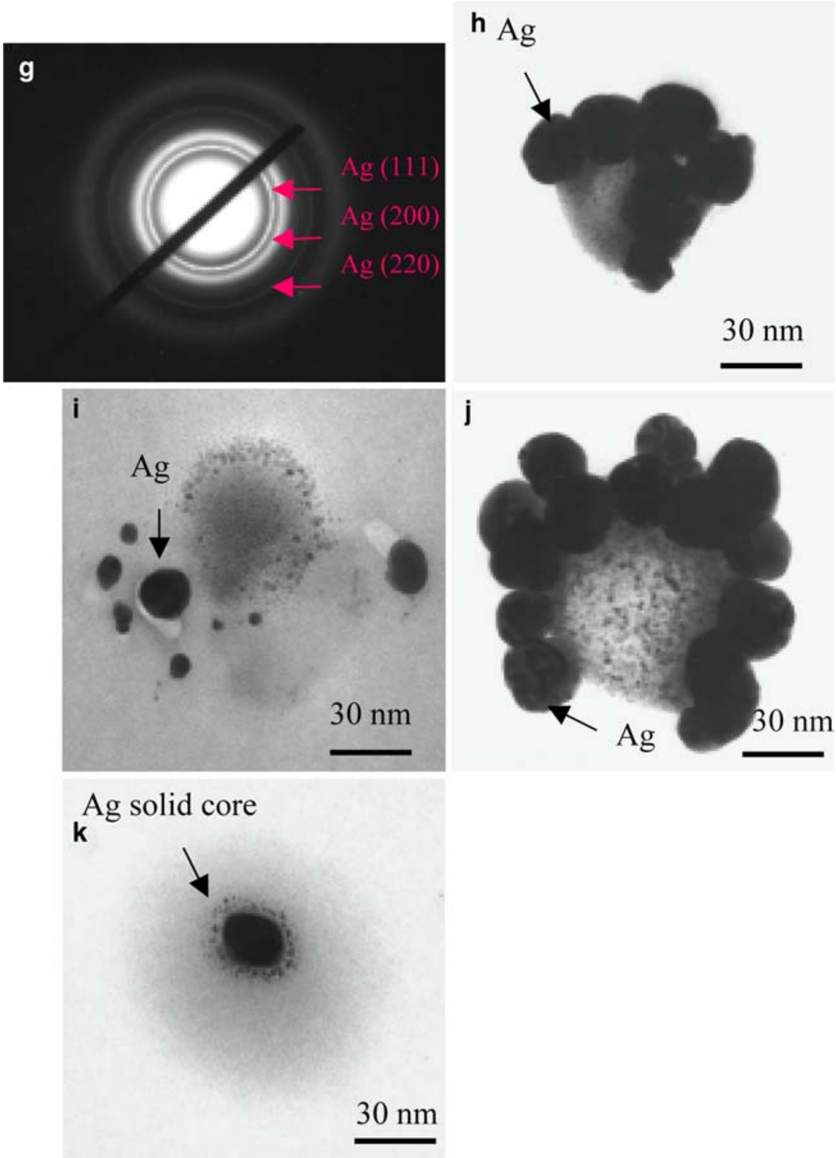

from sample MCP0.1. It is clear that these Ag-micelles were in a vesicular structure, and the lighter part of this is likely a trace of hydrocarbon constituent swollen by the formic acid. The Ag-micelles prepared from the sample MCP0.3 displayed two morphological types: the vesicle and the ring-like, as identified in Fig. 6b,c, respectively. In Fig. 6c, a dense crystalline Ag-shell is seen enclosing the micelle and no aggregate of Ag particles was found in the corona region.

The Ag-micelles in Fig. 5b were prepared from sample MCP0.5 and their enlarged TEM images are shown in Fig. 6d–f. Some were ring-like with aggregates of Ag particles, and most were the more commonly found star-like as shown in Fig. 6f. The extrusions of this star-like micelle were crystalline Ag particles as identified by the result of electron diffraction shown in Fig. 6g. By comparing Fig. 6e with f, it can be seen that the ring-like micelle has a large core with a relatively short corona, but vice versa for the star-like micelle. All these micelles with vesicle-like, ring-like and star-like shapes displayed the same morphologies of the Ag-shell structure.

In the specimen prepared from the MCP1.0 micelle solution, most of the micelles were observed to have the Ag-shell structure with Ag particles surrounding the polymer-core, as shown in Fig. 6h. The isolated Ag particles, as shown in Fig. 6i, which were very likely detached from the polymer-core due to specimen preparation were also observed. Figure 5c is the TEM image of Ag-micelles prepared from the sample MCP2.0, and an enlarged one is given in Fig. 6j. It can be seen that the

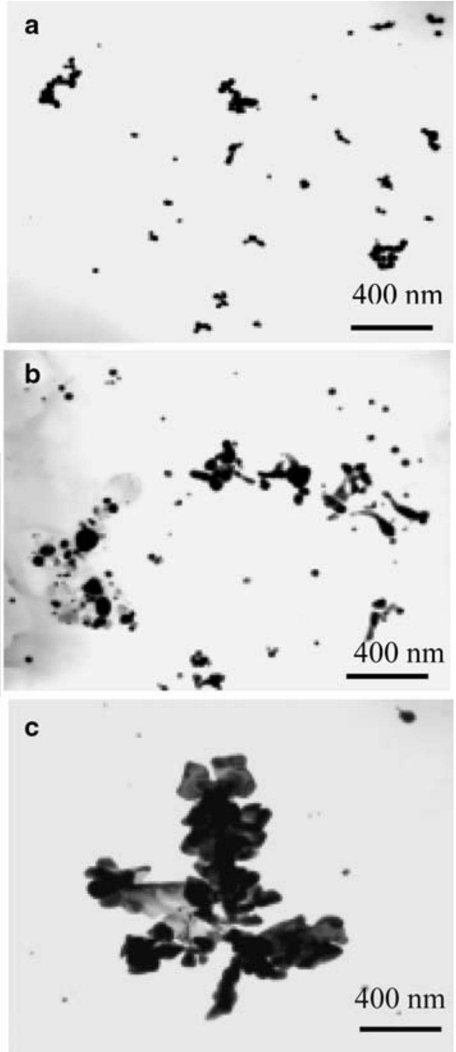

**Fig. 7** TEM images of dried specimens of $AgNO_3/HCOOH/H_2O$ systems, cast on a formval/carbon-coated copper grid. **a** 0.1 wt%$AgNO_3$; **b** 0.5 wt% $AgNO_3$; and **c** 1.0 wt% $AgNO_3$

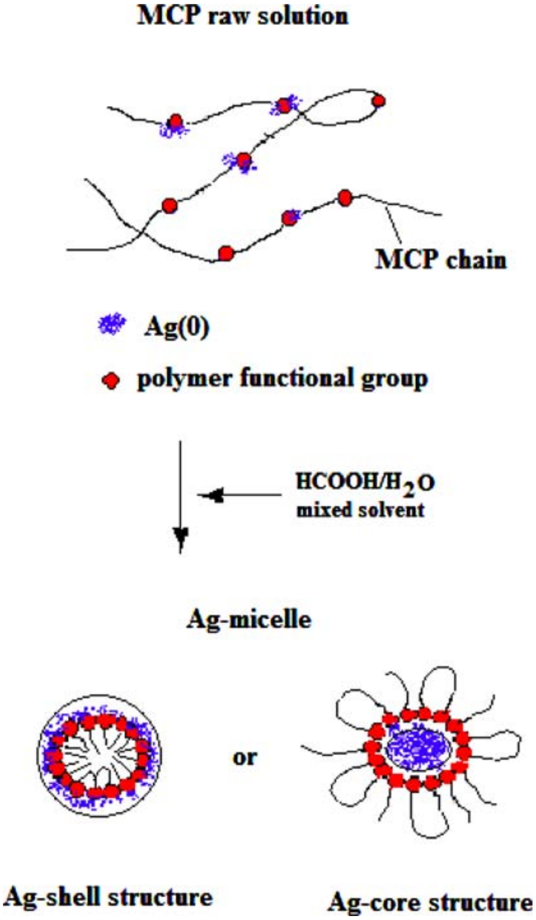

**Fig. 8** Schematic illustration for the model of the MCP micelle formation

micelle has a polymer-core surrounded by Ag particles, a structure similar to that shown in Fig. 6h of the MCP0.1 micelle. In this MCP2.0 system, the Ag-shell micelle was rarely observed. However, the individual Ag particles, as shown in Fig. 6k, which had a Ag-core structure surrounded by a "cotton-like" polymer were usually observed.

Figure 7 shows the TEM images of Ag particles formed in $AgNO_3/HCOOH/H_2O$ systems with the absence of PVAc, and it can be seen that the size and shape of these Ag particles varied with the added concentration of $AgNO_3$. As shown in Fig. 7a, most of the Ag particles that generated in the 0.1 wt% $AgNO_3$ system were spherical in shape and some aggregated to form short chains; but in Fig. 7b, the Ag particles formed in this 0.5 wt% $AgNO_3$ system displayed irregular shape and flocculation occurred, and in Fig. 7c the aggregated Ag particles of this 1.0 wt% $AgNO_3$ system even folded to form large crystals of polygonal shape.

By comparing the TEM results of both the MCP/$HCOOH/H_2O$ and $AgNO_3/HCOOH/H_2O$ systems, the Ag particles generated in MCP condition had regular shape and narrower size distribution, but the Ag particles formed in the absence of polymer became irregular in shape and even flocculated to form large crystals. Therefore, the result reveals that the PVAc polymer played an important role in controlling the morphology and also prevented the flocculation of Ag particles reduced by the HCOOH solvent.

## Model for micelle formation

Figure 8 depicts the micellization of MCP raw solution after the introduction of $HCOOH/H_2O$ mixed solvent. In this model the micelle has its core formed by the

**Table 3** The mean diameter of Ag-shell micelle and Ag-core micelle prepared from MCP micelle solution

| Sample | Ag-shell micelle Average size (nm) (SD) | Ag-core micelle Average size (nm) (SD) | Ag particle Average size (nm) (SD) |
|---|---|---|---|
| Pure PVAc | 58.88(79.72)[a] | – | – |
| MCP0.1 | 64.71(30.11) | – | –[b] |
| MCP0.3 | 74.28(16.35) | – | –[b] |
| MCP0.5 | 88.29(25.80) | – | 24.99(8.43)[c] |
| MCP1.0 | 121.24(25.41) | 67.50(14.35) | 16.87(8.17)[c] |
| MCP2.0 | 155.62(49.14) | 75.90(18.16) | 41.25(9.93)[d] |

[a] The PVAc micelles with irregular shape and broad size distribution

[b] All the MCP micelles have a Ag-shell morphology, in the shell range the metal nanoparticles are not agglomerated

[c] In the shell range of Ag-shell micelle, the size of agglomerated Ag nanoparticle

[d] The size of solid core of Ag-core micelle

polymer's hydrocarbon backbone and its corona contributed by the polymer's hydrophilic groups. The hydrophilic groups are the hydrolyzed hydroxyl groups of the polymer chain that have oxygen species capable of binding with the Ag constituent. Therefore the micelle generated in this $HCOOH/H_2O$ medium will be enclosed by an Ag-shell unless excessive Ag crystals or particles have aggregated to change the hydrophilic area to a hydrophobic one.

### Interaction of polymer-Ag particles in the MCP micelle

The results of TEM investigation demonstrated that Ag-micelles, when prepared from MCP raw solutions with different $AgNO_3$ concentrations, could exhibit variant morphological features. These results also suggest that two important factors, the Ag(0) content and the water affinity of the polymer chain, were dominant in affecting the variant morphology of these Ag-micelles. From the mean diameters of micelles and Ag particles that are summarized in Table 3, the effect of the Ag(0) content is apparent; the higher the $AgNO_3$ concentration in the MCP raw solution, the more the reduced Ag(0) constituent that were generated, and the formed Ag-micelles displayed variant morphology in the resultant micelle solution. It shows that micelles of Ag-shell structure were the main species generated in MCP raw solution of $AgNO_3$ concentration within 0.1–0.5 wt%. These Ag-shell micelles had their Ag(0) constituent attached at the corona region in the form of crystals or aggregate of particles, and their average size increased with the increasing $AgNO_3$ concentration. When the $AgNO_3$ concentration was increased above 0.5 wt%, the water affinity of the corona region began to decrease due to over-aggregation of Ag(0) particles, and thus the corona region became insoluble in the aqueous medium of the $HCOOH/H_2O$ solvent. The decrease in solubility forced the MCP chains to transform themselves into micelles of Ag-core structure, and the polymer chain was then swollen by formic acid to form the micellar corona. Ag-core micelles were usually found in MCP micelle solution prepared from a MCP raw solution with $AgNO_3$ concentration of 1.0–2.0 wt%, and the average size of Ag particles generated was smaller than 50 nm.

## Conclusions

The use of MCP raw solutions, simply prepared from PVAc polymer and silver nitrate, to generate Ag(0)-micelles of regular shape and narrow size distribution has been demonstrated in this study. The MCP micelle solutions induced by the right composition of $HCOOH/H_2O$ mixed solvent were thermodynamically stable and could stand at least for several months without precipitation. The morphology of the Ag-micelles was affected by the $AgNO_3$ concentration of the MCP raw solution. In the TEM investigation, the micelles with Ag-shell structure were usually found in MCP micelle solutions prepared from MCP raw solutions of $AgNO_3$ concentration within 0.1–0.5 wt%. There were variants in this Ag-shell structure, namely the vesicular, the ring-like, the star-like and the spherical. The size of these Ag-shell micelles was increased with the increasing concentration of $AgNO_3$. But when the $AgNO_3$ content was increased to 1.0–2.0 wt%, the micelles generated were transformed to Ag-core structure, which had the Ag solid particles enclosed within the polymer chains, and the size of these Ag particles was also increased with the increasing concentration of $AgNO_3$. The results of the TEM analysis also demonstrated that the polymer matrix of the MCP system, which functioned as a protecting agent, was effective in limiting the growth of the Ag particle size so that the flocculation of Ag particles was inhibited.

## References

1. Holmberg K, Jönsson B, Kronberg B, Lindman B (2002) Surfactants and polymers in aqueous solution, 2nd edn. Wiley, England, pp 261–303
2. Fendler JH (1998) Nanoparticles and nanostructured films-preparation, characterization and applications. Wiley, New York, pp 145–171
3. Riess G (2003) Prog Polym Sci 28:1107–1170
4. Zhang W, Shi L, An Y, Gao L, Wu K, Ma R, He B (2004) Phys Chem Chem Phys 6:109–115
5. Chen CW, Serizawa T, Akashi M (2002) Chem Mater 14:2232–2239
6. Zhao H, Douglas EP (2002) Chem Mater 14:1418–1423
7. Rheingans O, Hugenberg N, Harris JR, Fischer K, Maskos M (2000) Macromolecules 33:4780–4790
8. Monzen M, Kawakatsu T, Doi M, Hasegawa R (2000) Comput Theor Polym Sci 10:275–280
9. Carrot G, Valmalette JC, Plummer CJG, Scholz SM, Dutta J, Hoffmann H, Hilborn JG (1998) Colloid Polym Sci 276:853–859
10. Mayer ABR (1998) Mater Sci Eng C6:155–166
11. Ding J, Liu G, Yang M (1997) Polymer 38(21):5497–5502
12. Mössmer S, Spatz JP, Möller M, Aberle T, Schmidt J, Burchard W (2000) Macromolecules 33:4791–4798
13. Bronstein LM, Sidorov SN, Gourkova AY, Valetsky PM, Hartmann J, Breulmann M, Cölfen H, Antonietti M (1998) Inorganica Chim Acta 280:348–354
14. Lei L, Gohy JF, Willet N, Zhang JX, Varshney S, Jérôme R (2004) polymer 45:4375–4381
15. Choucair A, Eisenberg A (2003) Eur Phys J E 10:37–44
16. Hou S, Man KYK, Chan WK (2003) Langmuir 19:2485–2490
17. Aoki T, Muramatsu M, Torii T, Sanui K, Ogata N (2001) Macromolecules 34:3118–3119
18. Kim HS, Ryu JH, Jose B, Lee BG, Ahn BS, Kang YS (2001) Langmuir 17:5817–5820
19. Fang X, Yang C (1999) J Colloid Interface Sci 212:242–251
20. Shiraishi Y, Toshima N (1999) J Mol Catal A Chem 141:187–192
21. Huang CJ, Shieu FS (2003) Jpn J Appl Phys 42:5336–5341